Electronic Supplementary Material (ESI) for ChemComm.

A highly luminescent entangled metal-organic framework based on pyridine-substituted tetraphenylethene for efficient pesticide detection

Chen-Lei Tao,[‡a] Bin Chen,[‡b] Xun-Gao Liu,*[a] Li-Jiao Zhou,[a] Xiao-Li Zhu,[a] Jun Cao,[a] Zhi-Guo Gu,[c] Zujin Zhao,*[b] Liang Shen,[a] and Ben Zhong Tang[bd]

Table of Contents

S1. Materials and Methods

All chemicals and all solvents were purchased from commercial sources and used without further purification. ^{1}H NMR and ^{13}C NMR spectra were recorded on a Varian Unity 600 MHz and 150 MHz spectrometer. Mass spectra were recorded on an Agilent 6210TOF-MS spectrometer using electrospray ionization. The infrared spectra were recorded on a Shimadzu IR Prestige-21 FT-IR Spectrometer with pressed KBr pellets. UV-vis absorption spectra were recorded on PerkinElmer Lambda 750. X-ray crystal structure was obtained by using Bruker D8 CMOS detectors. The powder XRD patterns were recorded on a Bruker D8 ADVANCE X-ray diffractometer. Data was collected from 5°–50° 2θ, with the operating power set to 40 kV/40 mA. Thermal analyses were performed in nitrogen in the temperature range 25–650 ^{o}C with a heating rate of 10 $^{\circ}C$ min^{-1} on a GA-500 instrument. Fluorescence spectra were recorded on a Perkin-Elmer LS 55 spectrofluorometer. Solid fluorescence quantum yields were measured using a Hamamatsu absolute PL quantum yield spectrometer C11347 Quantaurus-QY. Fluorescence lifetimes were determined with a Hamamatsu C11367-11 Quantaurus-Tau time-resolved spectrometer. Theory calculations were using the density functional theory (DFT) with the B3LYP hybrid functional.

S2. Synthetic procedures

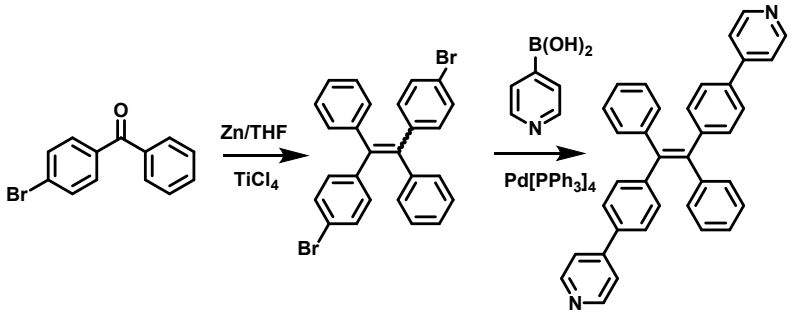

Scheme S1. Schematic representation of the synthesis strategy for BPyTPE.

Synthesis of 1,2-bis(4-bromophenyl)-1,2-diphenylethene (2Br-TPE): The synthesis of 1,2-bis(4-bromophenyl)-1,2-diphenylethene (2Br-TPE) was modified from the original reported procedures.[1,2] Zinc (16.8 mmol, 4.96 g) and 4-

bromobenzophenone (38.4 mmol, 10 g) were added in a flask. Then the flask was evacuated and charged with nitrogen for 3 times. The flask was filled with anhydrous tetrahydrofuran (THF, 100 mL) under stirring at –78 °C, and then filled with dichloromethane (DCM) solution of $TiCl_4$ (1 M, 42.8 mL). After stirring for 30 minutes, the solution was heated to reflux for 6 h under nitrogen. After cooling down to room temperature, the reaction was poured into water and extracted with DCM for three times. The combined organic layers were washed with water and potassium carbonate, and then dried over anhydrous magnesium sulfate. After filtration and solvent evaporation, the residue was purified by column chromatography using petroleum ether as eluent. White powder of 2Br-TPE was obtained in 70% yield. ^{1}H NMR (300 M Hz, $CDCl_3$), δ (TMS, ppm): 7.19-7.13 (m, 4H), 7.07-7.02 (m, 6H), 6.93-6.89 (m, 4H), 6.84-6.77 (m, 4H). ^{13}C NMR ($CDCl_3$, 75 MHz), δ (TMS, ppm): 141.84, 141.30, 139.25, 131.85, 130.14, 129.87, 126.99, 126.79, 125.96. HRMS: *m/z* = 490.2 $[M + H]^+$.

Synthesis of (*E*)-1,2-diphenyl-1,2-bis(4-(pyridin-4-yl)phenyl)ethene (BPyTPE): 2Br-TePE (1.020 mmol, 0.5 g) and (4-(pyridin-4-yl) phenyl) boronic acid (7.61 mmol, 0.94 g) was added in flask with evacuated and nitrogen for three times. Toluene (40 mL) and a solution of potassium carbonate (0.56 g, 0.95 mmol) in the mixture (10 mL) of ethanol and water (1:1, v/v) were then added. This reaction was catalyzed by tetrakis(triphenylphosphine)palladium (0.18 g, 0.152 mmol). The mixture was kept to reflux for 12 h. After cooling down to room temperature, the reaction was poured into water and extracted with DCM for three times. The combined organic layers were washed with water and potassium carbonate, and then dried over anhydrous magnesium sulfate. After filtration and solvent evaporation, the residue was purified by column chromatography using ethyl acetate/chloroform (4:1 v/v) as eluent. Pale yellow powder of BPyTPE was obtained in 25% yield. ^{1}H NMR (300 M Hz, $CDCl_3$), δ(TMS, ppm): 8.55 (d, J = 4.69 Hz, 4H), 7.41 (d, J = 5.18 Hz, 4H), 7.30-7.38 (m, 4H), 7.05-7.14 (m, 10H), 7.03 (dd, J = 7.32, 1.21 Hz, 4H). ^{13}C NMR ($CDCl_3$, 75MHz), δ (TMS, ppm): 150.10, 147.75, 144.62, 143.19, 140.91, 135.96, 132.11, 131.36, 128.48,

128.01, 126.94, 126.21, 121.32. ESI (FAB): *m/z* = 487.2 $[M + H]^+$.

Synthesis of complex 1

In a 2 mL glass bottle, $Zn(NO_3)_2 \cdot 6H_2O$ (5 mg, 16.8 μmol), biphenyl-4,4′-dicarboxylic acid (H_2bpdc, 2.7 mg 11.1 μmol), BPyTPE (5.4 mg, 11.1 μmol) were added with *N*,*N*-dimethylformamide (1 mL) and *N*,*N*-dimethylacetamide (50 μL). The reaction mixture was kept under ultrasonication for 10 minutes. The glass bottle was tightened and kept at 120 °C for 12 h. The transparent light yellow plate crystals (complex **1)** were harvested after cooled to room temperature. Yield: 70%. IR: (KBr pellet, cm^{-1}): 3442 (m), 3050 (w), 1676 (s), 1661 (s), 1541 (m), 1492 (m), 1400 (s), 1225 (w), 1176 (w), 1007 (w), 841 (w), 771 (m), 724 (w), 703 (w).

Preparing of solvent-free 1

Complex **1** (200 mg) was immersed in DCM for 24 h, and then the supernatant was decanted and fresh DCM was replenished. This process was repeated for three times, and solvent-free **1** was obtained under vacuum condition at room temperature. Anal. Calcd for $C_{32}H_{21}NO_4Zn$: C, 70.02; H, 3.86; N, 2.55%. Found: C, 69.38; H, 3.69; N, 2.63%. IR: (KBr pellet, cm^{-1}): 3444 (w), 1694 (vw), 1469 (s), 1615 (s), 1538 (w), 1493 (w), 1408 (s), 1222 (w), 856 (w), 841 (w), 726 (m).

Fluorescence titration of solvent-free 1

Solvent-free **1** was added to DCM and the mixture was kept under vortex to form suspension (0.15 mg mL^{-1}). The fluorescence titration detections were performed by adding guest molecules into solvent-free **1** suspension. The initial photoluminescence (PL) spectrum of the suspension and spectra after each guest molecules addition were recorded. Each measurement was repeated by three times.

Crystallographic studies. Data collection for BPyTPE and complex **1** were carried out on a Bruker D8 CMOS detectors. Hemisphere of data were collected in the θ

range of 2.83-22.25 for BPyTPE and 0.85-25.40 for complex **1**, respectively. The data were integrated using the Siemens SAINT program,[3] with the intensities corrected for Lorentz factor, polarization, air absorption, and absorption due to variation in the path length through the detector faceplate. Empirical absorption and extinction corrections were applied. The structures were solved by direct method and refined on F^2 by full-matrix least squares using SHELXTL.[4] BPyTPEs are two-fold disordered ligands in complex **1**. There was an inversion center close to the middle of one BPyTPE, consisting of C8c-C25c, C8x-C25x, N1c and N1x atoms, the occupancy of which was therefore fixed to 0.5. The occupancy of the other BPyTPE was freely refined. The value of C9a-C25a, N1a, C9b-C25b and N1b were 0.82 and that of C9y-C25y, N1y, C9z-C25z and N1z were 0.18. Only C9a-C25a, N1a, C9b-C25b and N1b of the disordered atoms were anisotropically refined. All the atoms within or directly connected to the disordered aromatic rings were restrained to be flat. The thermal ellipsoids of disordered C9-C25 and N1 atoms were restrained to be similar. Distance restraints were also applied to these disordered atoms. Except for BPyTPE, other non-hydrogen atoms were refined anisotropically. All hydrogen atoms were put in calculated positions and refined isotropically with the isotropic vibration parameters related to the non-hydrogen atoms to which they are bonded. There were few A and B errors in checkCIF report of BPyTPE, which were resulted from disorder of phenyl rings. The solvent molecules are highly disordered, and attempts to locate and refine the solvent peaks were unsuccessful. These solvent molecules were removed using the SQUEEZE routine of PLATON and the structure was then refined again using the data generated.[5]

S3. Single crystal structure determinations

Table S1. Crystal data and structure refinements for BPyTPE.

Compound	BPyTPE	Complex **1**
Formula	$C_{36}H_{26}N_2$	$C_{32}H_{21}NO_4Zn$
M	486.59	548.87
crystal system	monoclinic	triclinic
space group	$P2_1$	$P\bar{1}$
a/Å	5.6957(4)	15.071(2)
b/Å	34.431(2)	15.109(2)
c/Å	13.1466(9)	24.650(4)
α/deg	90	84.430(5)
β/deg	90.142(2)	76.275(5)
γ/deg	90	83.485(5)
V/Å ^{3}	2578.1(3)	5403.2(13)
Z	4	6
temperature/K	173(2)	173(2)
λ(radiation wavelength)/Å	0.71073	0.71073
D(g/cm^3)	1.254	1.012
reflections collected	35464	60003
$R1^a$[I >2σ(I)]	0.1076	0.0690
$wR2^b$[I >2σ(I)]	0.2778	0.1703
goodness-of-fit	1.199	1.054
CCDC no.	1552085	1552086

$^aR1 = \sum|F_o - F_c|/\sum|F_o|$. $^bwR2 = [\sum[w(Fo^2 - Fc^2)^2]/w(Fo^2)^2]^{1/2}$

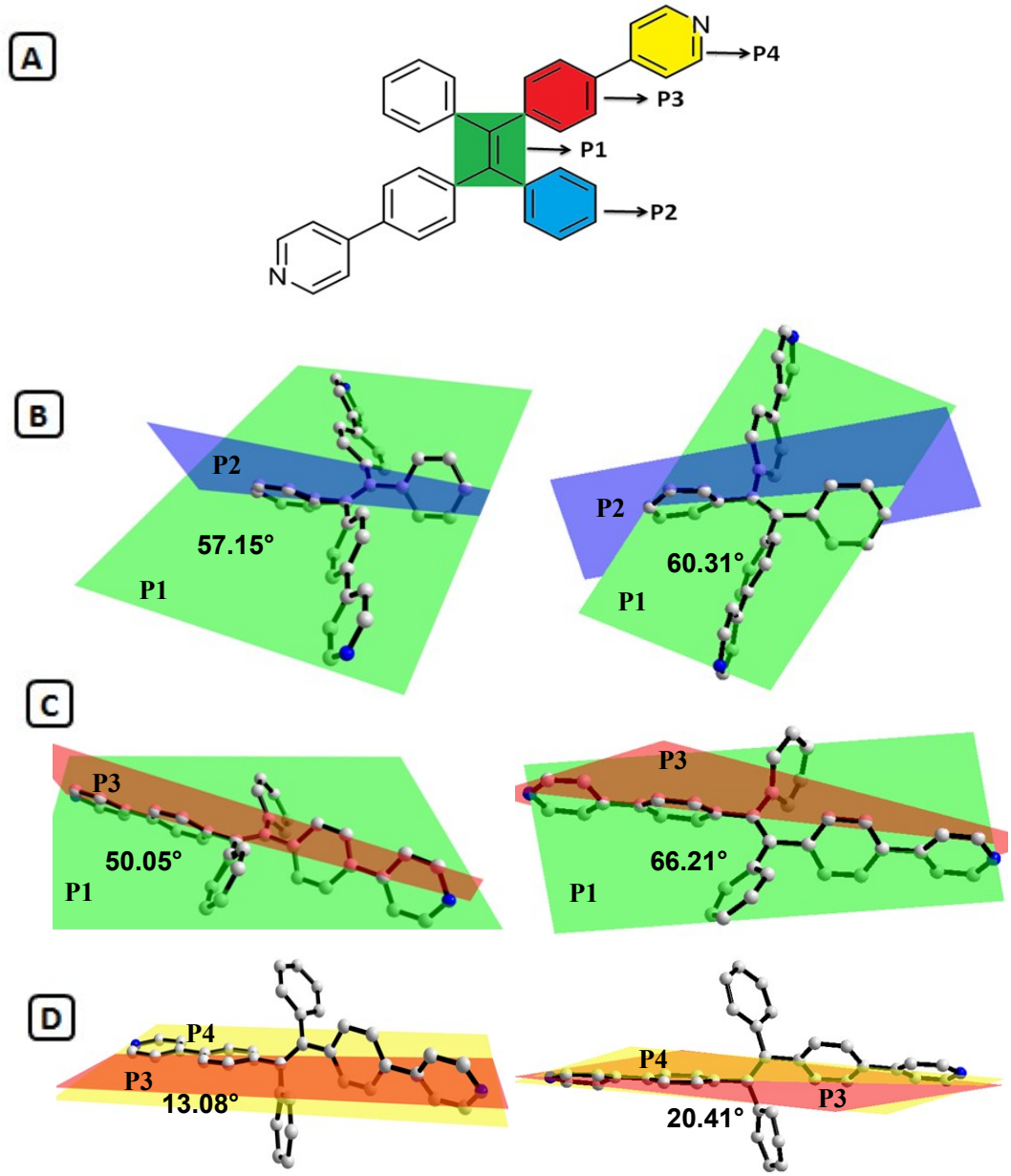

Fig. S1 (A) The plane of the two C atoms forming central C=C double bound and four C atoms surround them is named P1. The planes of free phenyl ring adjacent to C=C bond are named P2. The planes of phenyl ring connected with pyridine group are named P3. The plane of phenyl ring adjacent to pyridine group is named P4. The average dihedral angles are labeled for left column of (B) P1-P2, (C) P1-P3 and (D) P3-P4 in BPyTPE ligand. The average dihedral angles are labeled for right column of (B) P1-P2, (C) P1-P3 and (D) P3-P4 in complex **1**. All hydrogen atoms are omitted for clarity.

Table S2. The dihedral angles of BPyTPE in single crystals and in complex 1

	BPyTPE in single crystals	BPyTPE in complex **1**
P1-P2(°)	57.15	60.31
P1-P3(°)	50.05	66.21
P3-P4(°)	13.08	20.41

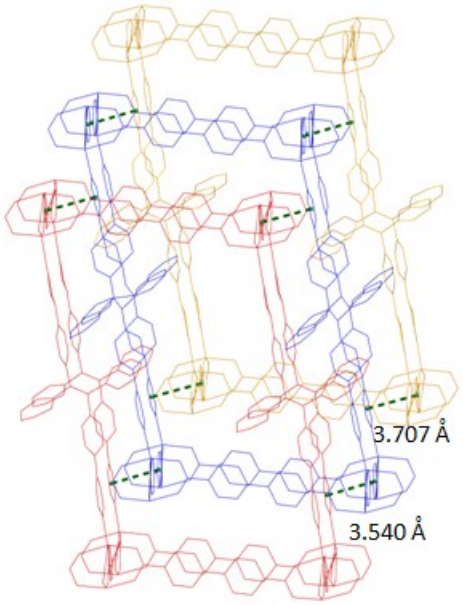

Fig. S2 π–π Stacking interactions of complex **1** (the green dotted lines are labeled for π–π interactions).

S4. Powder X-ray diffraction (PXRD) analysis

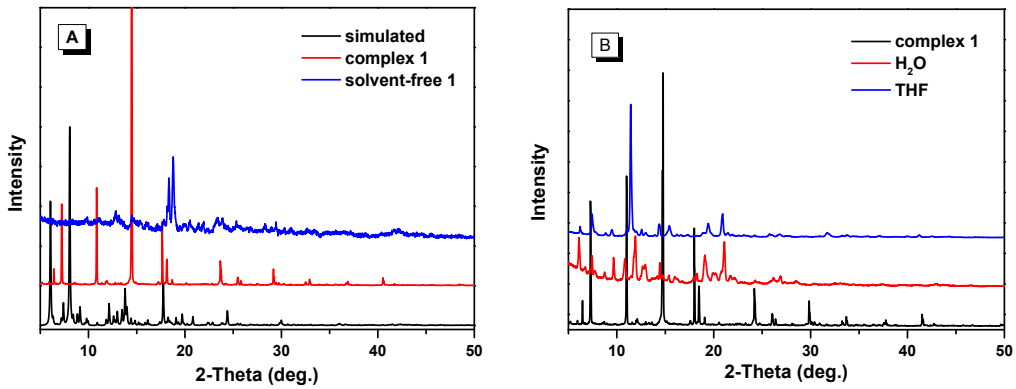

Fig. S3 (A) The PXRD patterns of simulated (black), complex **1** (red), and solvent-free **1** (blue). (B) PXRD patterns of complex **1** after soaked into H_2O (red) and THF (blue).

S5. Thermogravimetric analysis

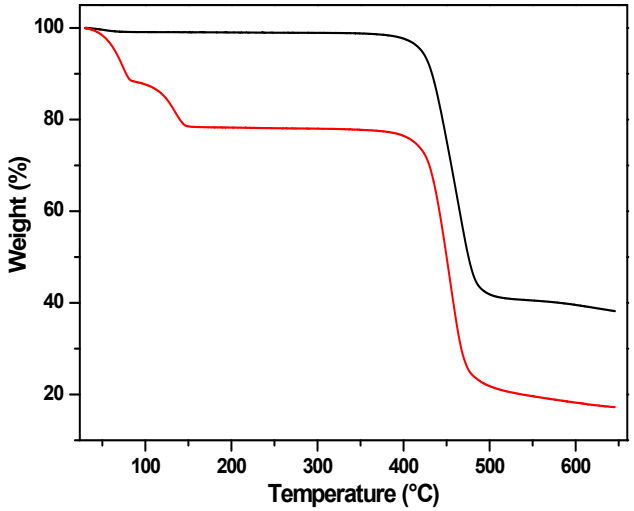

Fig. S4 Thermogravimetric analyses of complex **1** (red) and solvent-free **1** (black).

S6. Optical data

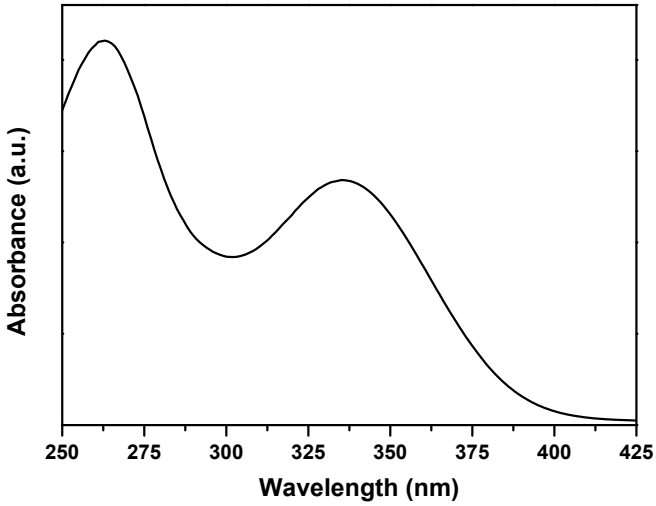

Fig. S5 UV-vis absorption spectrum of BPyTPE in THF solution.

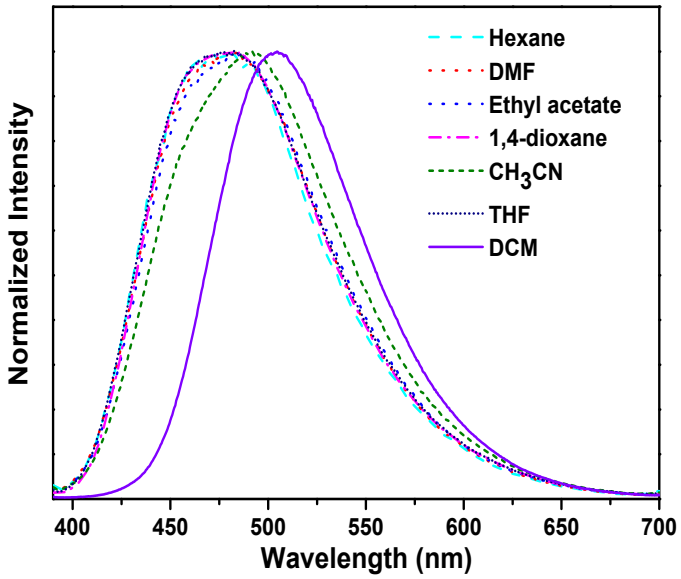

Fig. S6 Emission spectra of solvent-free **1** dispersed in different solvent (λ_{ex} = 365 nm).

Table S3. Fluorescence emission wavelengths of solvent-free **1** dispersed in different solvents.

solvent	λ_{max} (nm)
Hexane	480.5
DMF	485.5
Ethyl acetate	483.0
1,4-dioxane	479.5
CH3CN	492.0
THF	476.5
DCM	504.0

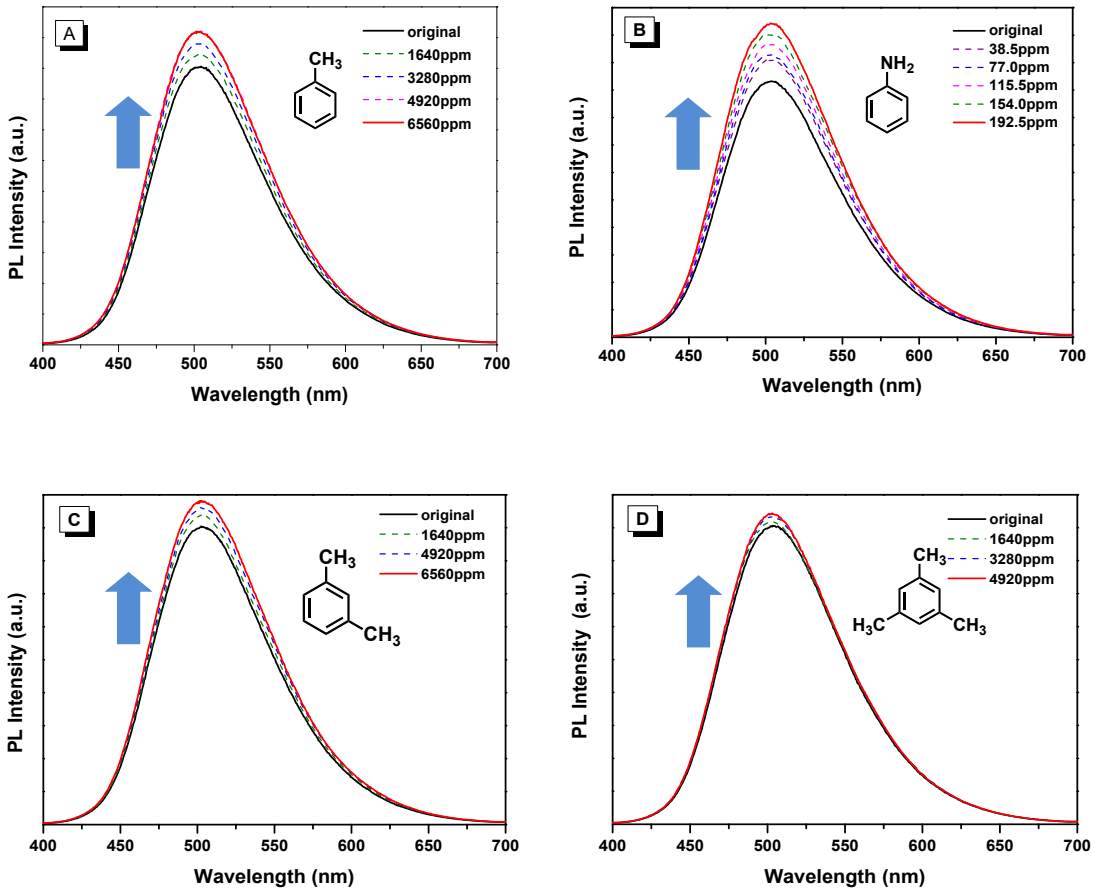

Fig. S7 (A) Fluorescence titration of solvent-free **1** in DCM suspension with varied concentrations of toluene. (B) Fluorescence titration of solvent-free **1** in DCM suspension with varied concentrations of aniline. (C) Fluorescence titration of solvent-free **1** in DCM suspension with varied concentrations of *m*-xylene. (D) Fluorescence titration of solvent-free **1** in DCM suspension with varied concentrations of mesitylene (λ_{ex} = 365 nm).

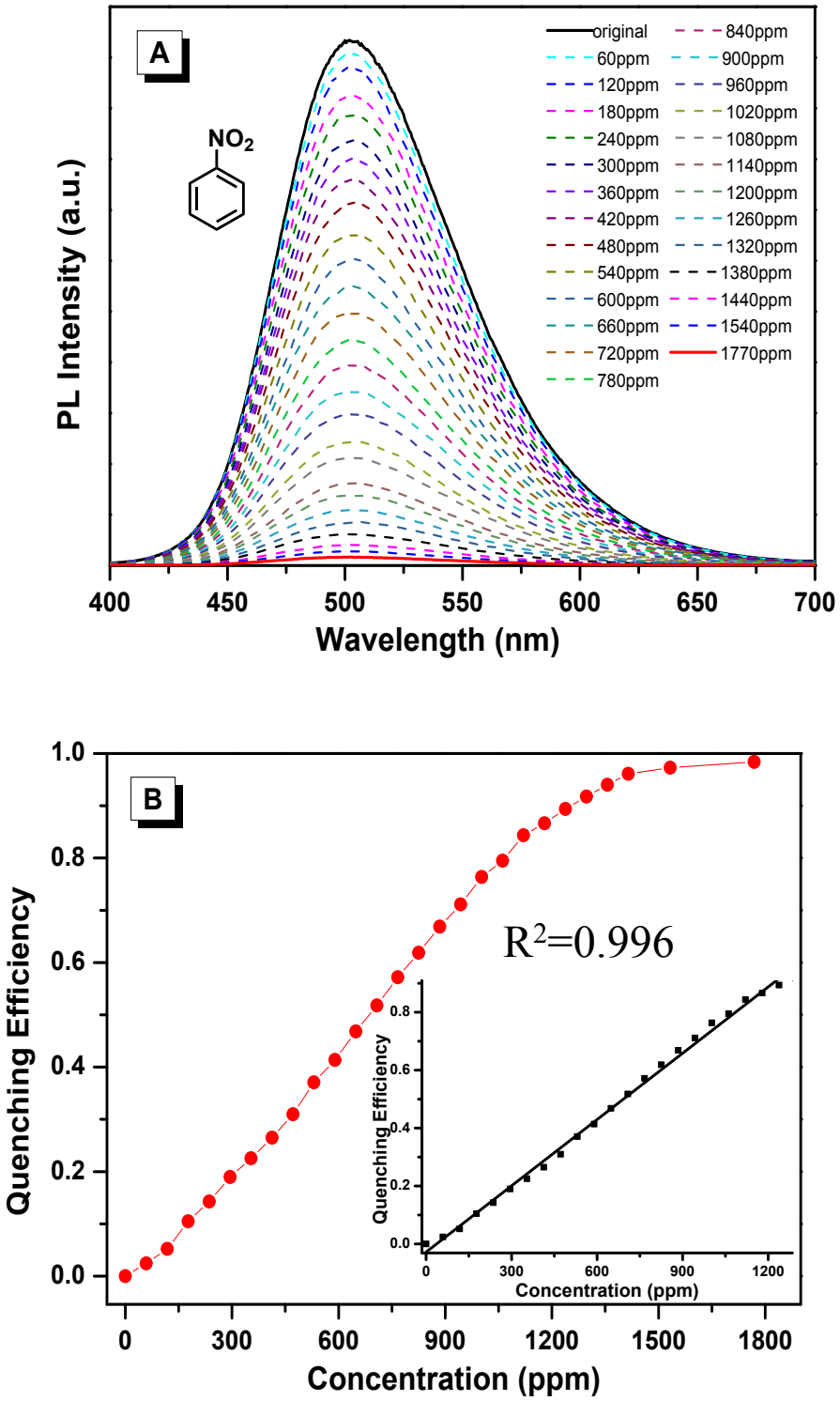

Fig. S8 (A) Fluorescence titration of solvent-free **1** in DCM suspension with varied concentrations of nitrobenzene (λ_{ex} = 365 nm). (B) Correlation between the quenching efficiency and concentration of nitrobenzene. Inset: the linear relationship of fitting (0–1300 ppm).

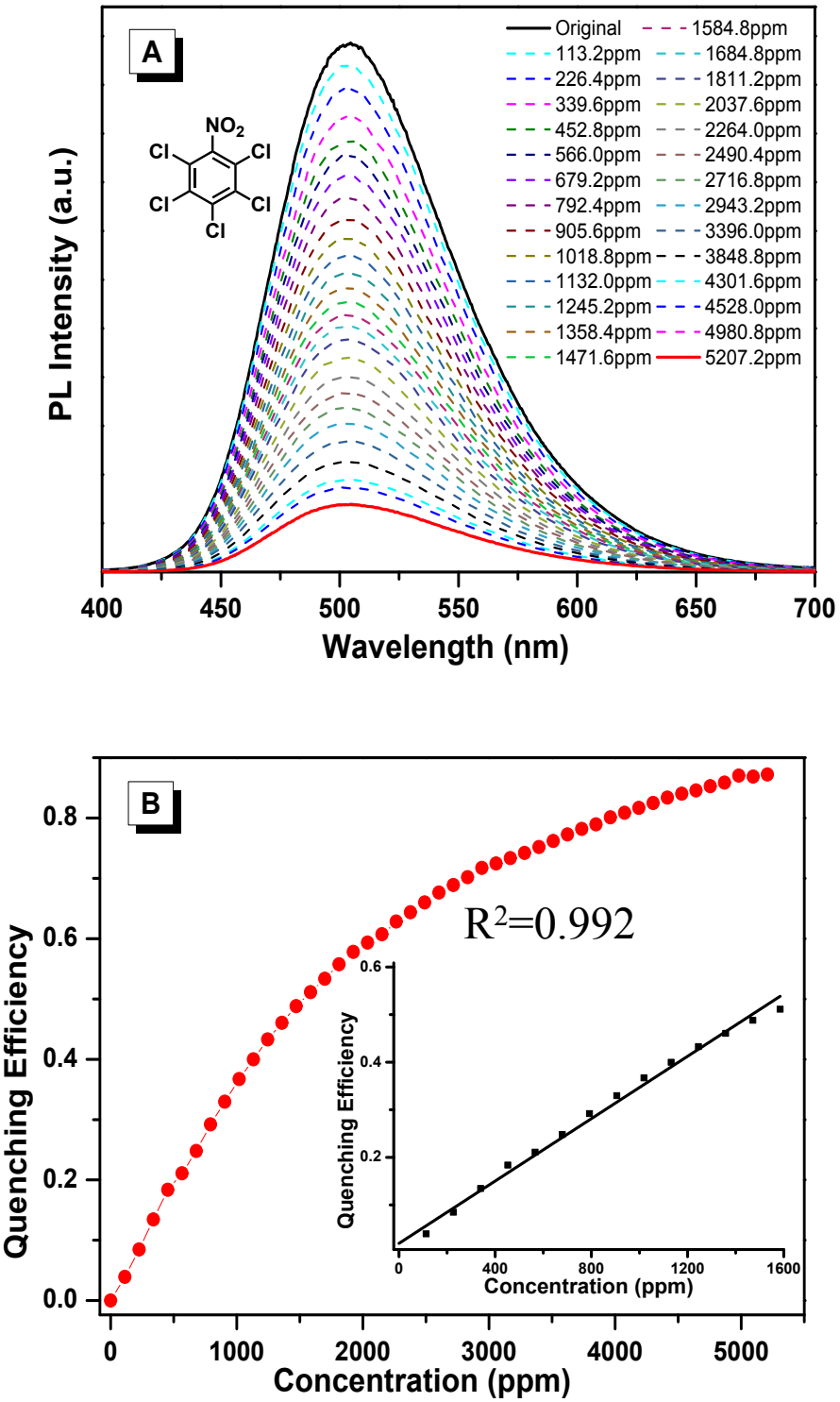

Fig. S9 (A) Fluorescence titration of solvent-free **1** in DCM suspension with varied concentrations of 1,2,3,4,5-pentachloro-6-nitrobenzene (λ_{ex} = 365 nm). (B) Correlation between the quenching efficiency and concentration of 1,2,3,4,5-pentachloro-6-nitrobenzene. Inset: the linear relationship of fitting (0–1600 ppm).

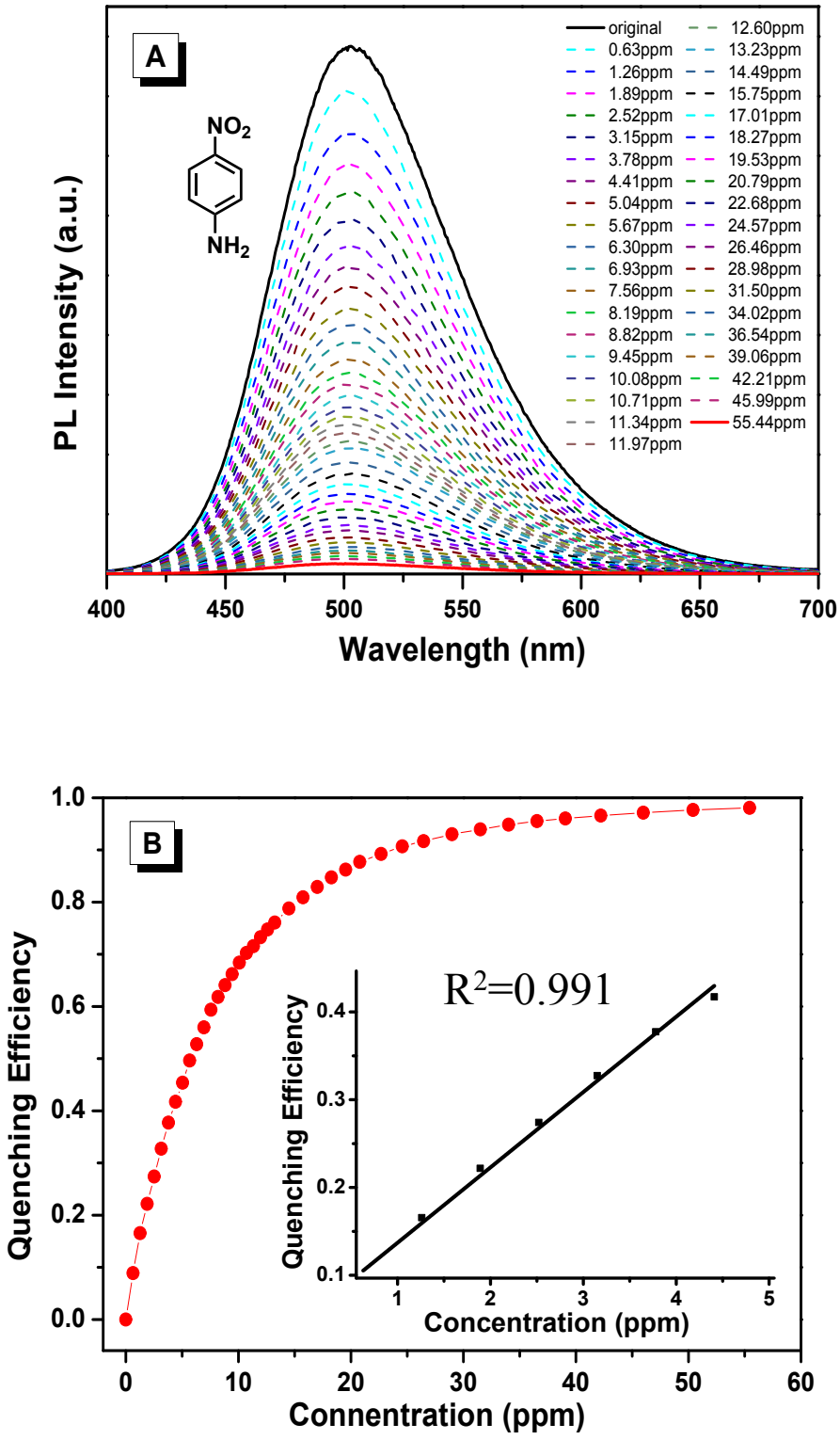

Fig. S10 (A) Fluorescence titration of solvent-free **1** in DCM suspension with varied concentrations of 4-nitroaniline (λ_{ex} = 365 nm). (B) Correlation between the quenching efficiency and concentration of 4-nitroaniline. Inset: the linear relationship of fitting (0–5 ppm).

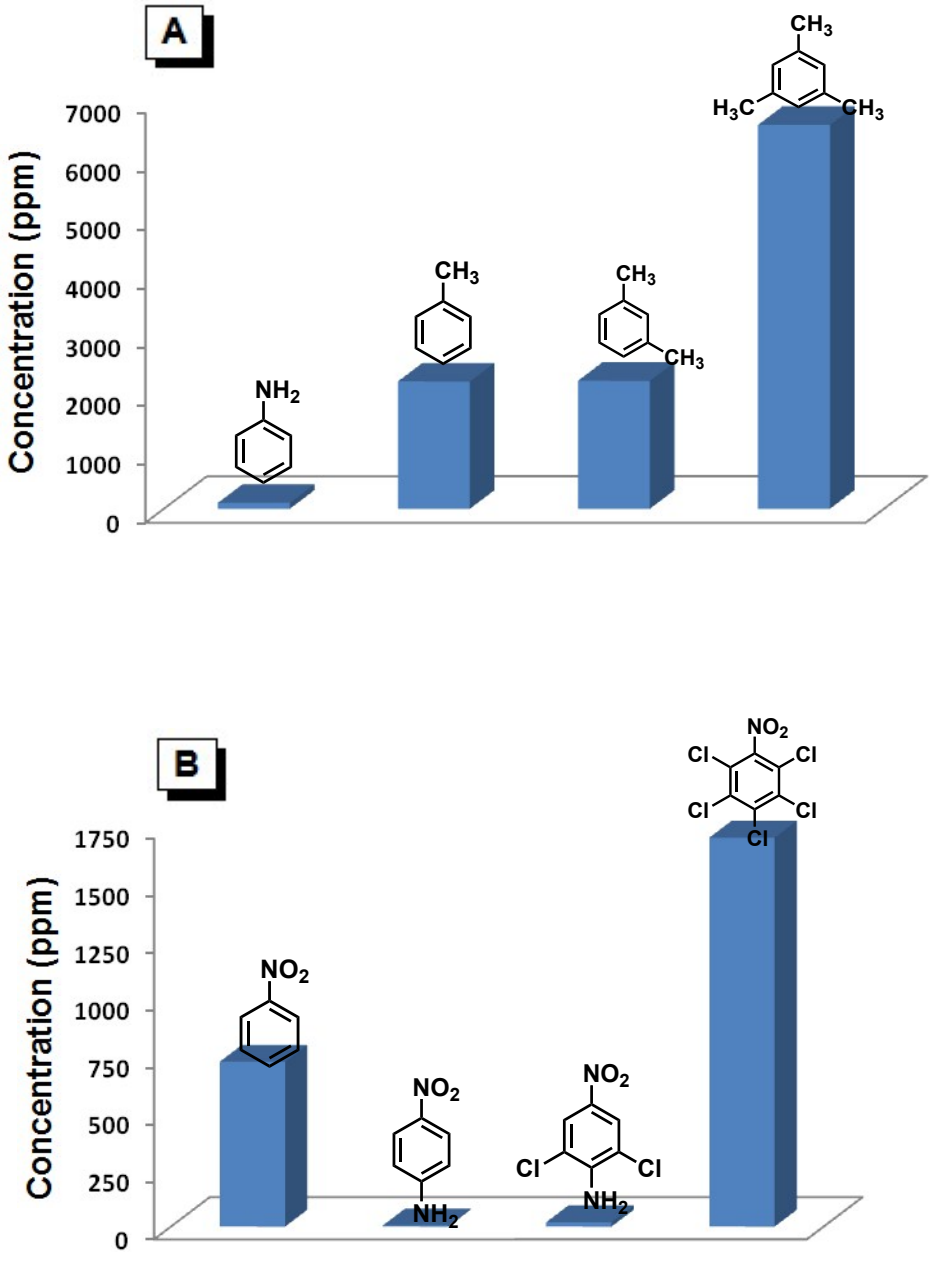

Fig. S11 (A) The concentration of fluorescence intensity increased by 4 %; (B) The concentration of fluorescence intensity decreased by 50%.

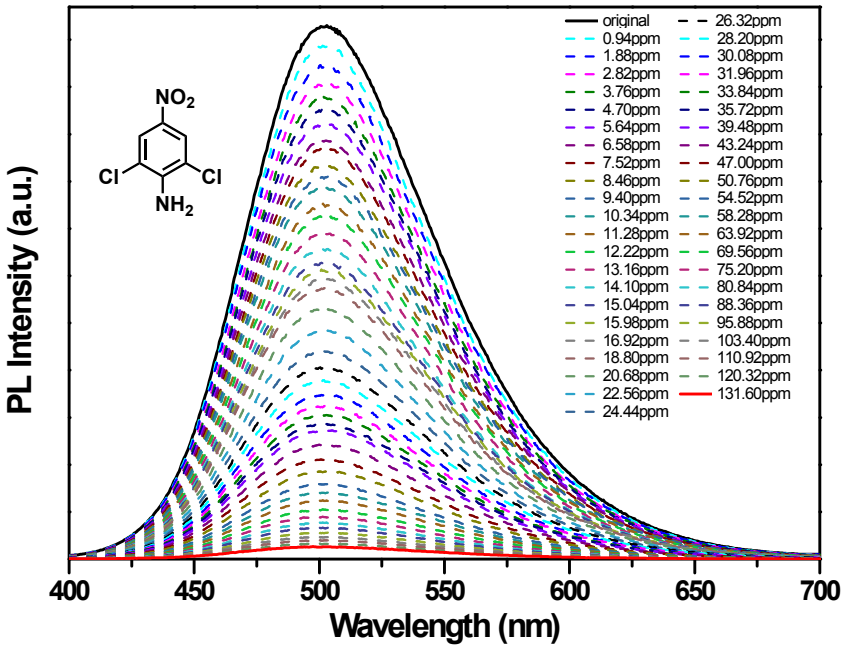

Fig. S12 (A) Fluorescence titration of solvent-free **1** in DCM suspension with varied concentrations of 2,6-dichloro-4-nitroaniline (λ_{ex} = 365 nm).

S7. Limit of detection (LOD) for pesticide

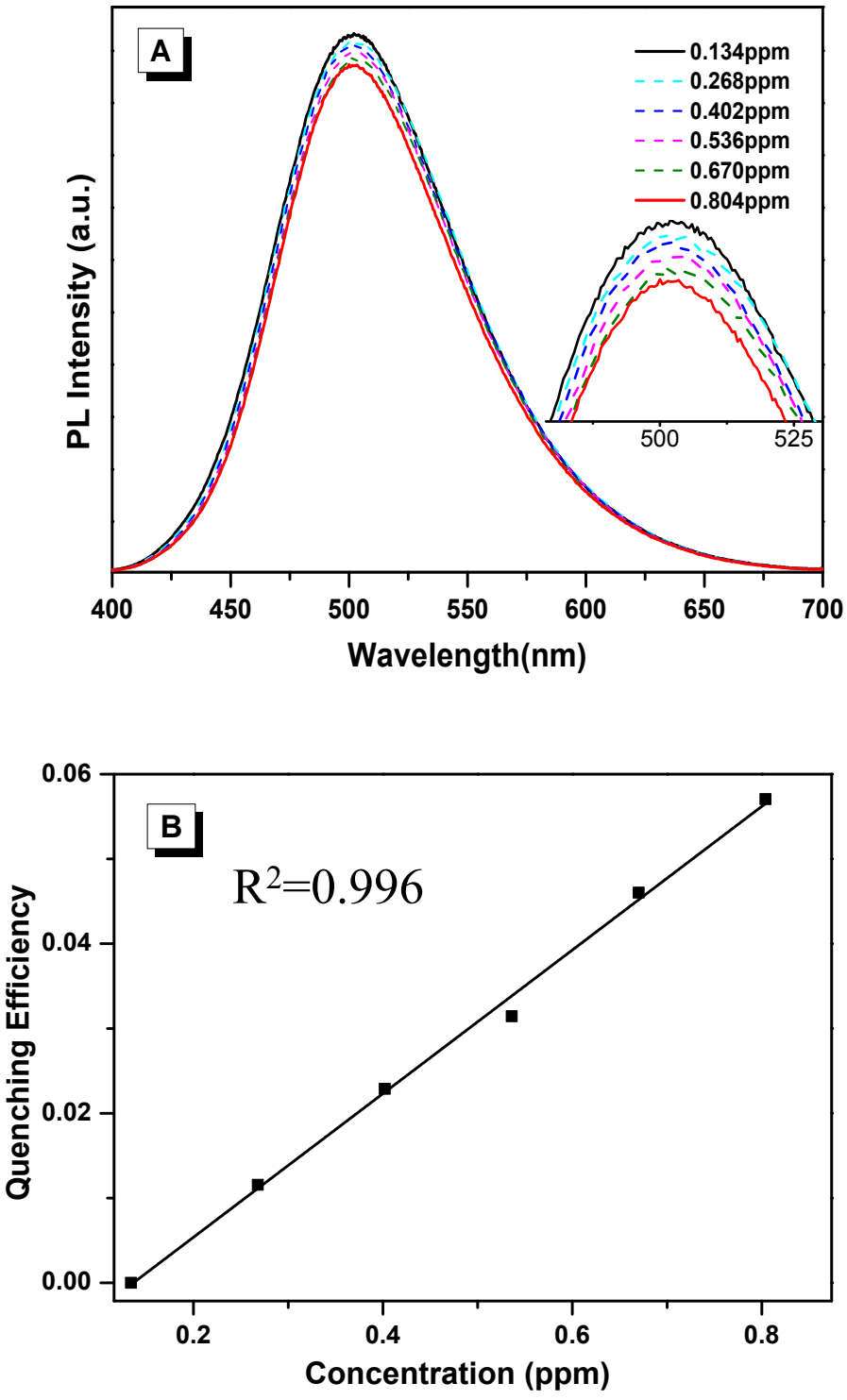

Fig. S13 (A) Low-concentration fluorescence titration of 2,6-dichloro-4-nitroaniline, with peak detail inset. (B) The fitting relationship for low-concentration fluorescence titration of solvent-free **1** with 2,6-dichloro-4-nitroaniline.

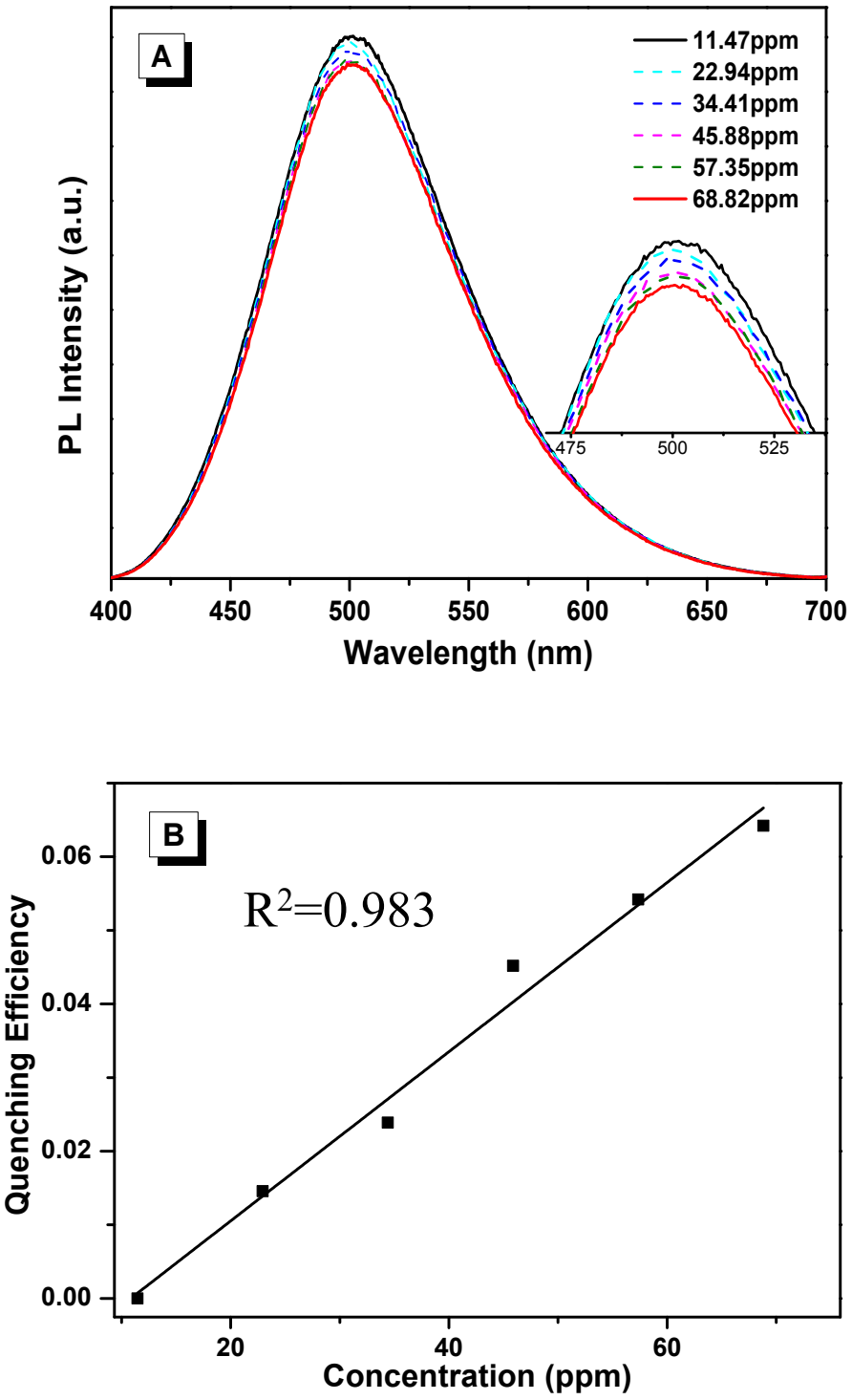

Fig. S14 (A) Low-concentration fluorescence titration of 1,2,3,4,5-pentachloro-6-nitrobenzene, with peak detail inset. (B) The fitting relationship for low-concentration fluorescence titration of solvent-free **1** with 1,2,3,4,5-pentachloro-6-nitrobenzene.

S8. Mechanism for fluorescence sensing

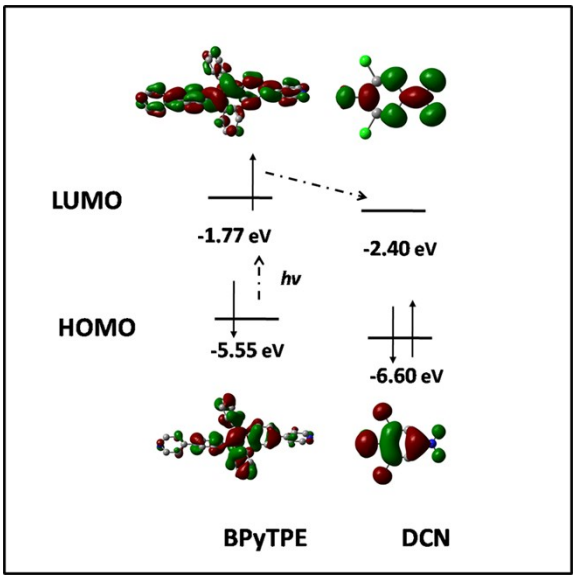

Fig. S15 The HOMO and LUMO energy levels of BPyTPE in complex **1** and DCN.

S9. Reference

1 K. R. Ghosh, S. K. Saha, J. P. Gao and Z. Y. Wang, *Chem. Commun*., 2014, **50**, 71–68.

2 Y. Ma, H. Ma, Z. Yang, J. Ma, Y. Su, W. Li and Z. Lei, *Langmuir*, 2015, **31**, 4916–4923.

3 S. K. Kurtz and T. T. Perry, *J. Appl. Phys.*, 1968, **39**, 3798.

4 SAINT, Program for Data Extraction and Reduction, Siemens Analytical X-ray Instruments, Madison, WI, 1994–1996.

5 SHELXTL (version 5.0), Reference Manual, Siemens Industrial Automation, Analytical Instruments, Madison, WI, 1995.